DE-FG05-80ET-53088-662 IFSR #662

Convective Amplification of Drift-Acoustic Waves in Sheared Flows

F.L. WAELBROECK, J.Q. DONG, W. HORTON,
and P.N. YUSHMANOV
Institute for Fusion Studies
The University of Texas at Austin
Austin, Texas 78712

August 1994

August 2, 1994

Convective amplification of drift-acoustic waves in sheared flows

F. L. Waelbroeck, J. Q. Dong, W. Horton, and P. N. Yushmanov

Institute for Fusion Studies, The University of Texas at Austin

Austin, Texas 78712

Abstract

The evolution of wavepackets is investigated in a cold-ion plasma model with sheared magnetic and velocity fields. Wavepackets may be amplified by the drift Kelvin-Helmholtz mechanism even when the velocity shear is such that normal modes are stable. It is shown that the logarithm of the convective amplification can be an order of magnitude greater than the logarithm of the steady-state amplification often taken as the measure of convective instability. For a given wavenumber, the maximum of either of these amplifications decreases only as the inverse of the perpendicular component of the velocity shear.

I. INTRODUCTION

It has recently been established that shear in the plasma flow velocity, when directed perpendicular to the magnetic field, has a stabilizing effect on the most common drift-acoustic instabilities.[1–5] This effect is counterintuitive, given that the velocity gradient constitutes a supplemental source of energy. It is understood by recalling that the existence of unstable eigenmodes requires the presence of a potential well capable of supporting a standing wave. The velocity shear acts by levelling this well, thereby increasing the energy necessary to establish a standing-wave pattern and thus stabilizing the eigenmodes.

Since the stabilization mechanism acts on the reflection properties of the waves, rather than on the mechanism driving the instability, one anticipates that fluctuations may continue to transport energy across the equilibrium gradients even in the absence of unstable eigenmodes. This seems particularly likely in applications where the spatial variation of the dielectric permittivity is weak, so that travelling wavepackets retain coherence during many periods of oscillation. In such applications, it can be argued that the stability of propagating waves is of greater relevance than that of eigenmodes.

The stability of propagating waves has traditionally been investigated by neglecting entirely the spatial variation of the permittivity, in a procedure referred to as the local analysis. The simplicity of this procedure permits the analysis of complicated but important kinetic effects.[6] The spatial variation of

the permittivity *does* play a role, however, in limiting the time during which a wavepacket may remain in resonance and receive energy from the plasma.[7,8] In order to judge the importance of wavepackets for transport, it is necessary to consider their *complete* evolution and the maximum amplification they may experience.

In the present paper, we describe a new technique for evaluating the amplification. Our technique is based on the observation that the weak spatial dependence allows two important simplifications. First, the method of phase-integrals may be used to determine the response to a localized, fixed-frequency excitation of the plasma (Greene's function).[7,8] Second, the method of stationary phase may be used to evaluate the inverse Laplace transform.

We apply our technique to evaluate the amplification of drift-acoustic wavepackets in a plasma with sheared equilibrium velocity. For simplicity, we consider the Drift-Kelvin-Helmholtz (DKH) instability in a cold-ion plasma:[9,10] this model allows both the eigenfunctions and the phase-integral (WKB) solutions to be evaluated exactly. The DKH eigenmodes have been shown to be stabilized when the perpendicular component of the velocity shear is greater than a critical threshold *independent of the (destabilizing) parallel component of the velocity shear.*[5] The critical velocity shear is such that the lateral phase velocity (perpendicular to $\mathbf{B}$ and $\boldsymbol{\nabla} n$) is constant. We recover this result here with the method of phase integrals. We then show

that substantial convective amplification may persist above the threshold for eigenmode stabilization, and that this amplification decreases only as the inverse of the perpendicular component of the velocity-shear.

This paper is organized as follows. We begin in Sec. II by formulating the initial value problem. In Sec. III, we describe the case where the coefficients of the wave equation are constant and the solutions consist of plane waves. The more general case of slowly varying coefficients (that is, of weak magnetic and flow shear) calls for the application of the method of phase integrals. We review this method in Sec. IV before applying it in Sec V to the study of eigenmodes. The steady-state and convective amplifications are then evaluated in Sec. VI. Section VII concludes with a discussion of our results.

II. THE INITIAL VALUE PROBLEM

We consider a plane slab geometry with a magnetic field and equilibrium flow velocity lying in the (y, z) plane and varying in the transverse direction x. The velocity shear vector is denoted by $\mathbf{W} = d\mathbf{V}/dx$, and the magnetic field is taken to be $\mathbf{B} = B_0(\hat{\mathbf{z}} + \hat{\mathbf{y}}\, x/L_s)$. The electron response is assumed to be adiabatic, $\tilde{n}_e = en_0\tilde{\phi}/T_e$, and the ion response is determined by the equations of continuity and momentum conservation,

$$\frac{\partial n_i}{\partial t} + \nabla \cdot (n_i \mathbf{V}_i) = 0 \,,$$

$$M_i \left(\frac{\partial \mathbf{V}_i}{\partial t} + \mathbf{V}_i \boldsymbol{\nabla} \mathbf{V}_i \right) = e \left(\mathbf{E} + \mathbf{V}_i \times \frac{\mathbf{B}}{c} \right) .$$

The rotation shear frequency is assumed to be comparable to the drift frequency in the standard drift-ordering, $W \sim \omega_* \ll \Omega_i$ and $L_n^{-1} \sim k_\parallel \ll k_\perp$, where $\omega_* = k_y v_D$ is the drift frequency and Ω_i is the gyrofrequency.

We linearize these equations and look for solutions of the form $\widetilde{\phi}(x,t) \exp[i(k_z z + k_y y)]$. The Laplace transform of the ion momentum equation is solved for the perturbed velocity $\overline{\mathbf{v}} = \overline{\mathbf{v}}_E + \overline{\mathbf{v}}_P + \overline{\mathbf{v}}_\parallel$, where

$$\overline{\mathbf{v}}(x,\omega) = \int_0^\infty dt\, \widetilde{\mathbf{v}}(x,t) e^{i\omega t}$$

for $\mathrm{Im}(\omega) > 0$. It follows

$$\overline{\mathbf{v}}_E(x,\omega) = \left(\frac{c}{B} \right) (\widehat{\mathbf{b}} \times \boldsymbol{\nabla}) \overline{\phi}(x,\omega) ,$$

$$\overline{\mathbf{v}}_P(x,\omega) = i \left(\frac{c}{\Omega_i B} \right) \left[(\omega_d \boldsymbol{\nabla} + k_y W_\perp \widehat{\mathbf{x}}) \overline{\phi}(x,\omega) + \boldsymbol{\nabla} \widetilde{\phi}(x,0) \right] ,$$

$$\overline{v}_\parallel(x,\omega) = \left[\left(\frac{c}{B} \right) (\Omega_i k_\parallel - k_y W_\parallel) \overline{\phi}(x,\omega) + \widetilde{v}_\parallel(x,0) \right] \Big/ \omega_d ,$$

where $\omega_d = \omega - \mathbf{k} \cdot \mathbf{V}(x)$ is the Doppler shifted frequency. Consistent with the drift ordering, all terms of order higher than first in the series-expansion of the Doppler shift are neglected:

$$\omega_d = \omega - \mathbf{k} \cdot \mathbf{V}(0) - k_y W_\perp x .$$

This approximation may be compared to the neglect of the transverse variation of the drift frequency in the investigations of static plasmas.[11] Henceforth, we will ignore the uniform Doppler shift $\mathbf{k}\cdot\mathbf{V}(0)$. Note that the effect of the second derivative of the equilibrium $\mathbf{v}_E$ on the local stability properties has been investigated by Migliuolo and Sen.[6]

Substituting these results into the Laplace transform of the continuity equation yields the initial value equation

$$\rho_s^2\frac{d^2\overline{\phi}}{dx^2}+\left(-(1+k_y^2\rho_s^2)+\frac{\omega_*}{\omega_d}-k_y\rho_s W_\parallel\frac{k_\parallel c_s}{\omega_d^2}+\frac{k_\parallel^2 c_s^2}{\omega_d^2}\right)\overline{\phi}=\Gamma(x,\omega)\ . \qquad (1)$$

The initial conditions enter through the function

$$\Gamma(x,\omega)=\frac{1}{i\omega_d}\left[\left(1+k_y^2\rho_s^2-\rho_s^2\frac{d^2}{dx^2}\right)\widetilde{\phi}(x,0)+\frac{T_e k_\parallel\widetilde{v}_\parallel(x,0)}{e\omega_d}\right]\ . \qquad (2)$$

Using ρ_s and $1/\omega_*$ as units of length and time, the initial value equation takes the form

$$\frac{d^2\overline{\phi}}{dx^2}+\left(-g_{ky}+\frac{1}{\omega_d}-w_\parallel\frac{sx}{\omega_d^2}+\frac{s^2x^2}{\omega_d^2}\right)\overline{\phi}=\Gamma(x,\omega)\ . \qquad (3)$$

where $g_{ky}=1+k_y^2\rho_s^2$; $\omega_d=\omega-w_\perp x$; $s=L_n/L_s$; $w_\perp=L_nW_\perp/c_s$ and $w_\parallel=L_nW_\parallel/c_s$. The most important feature of this equation is that the perpendicular component of the flow-shear appears *only* as a Doppler shift of the frequency; it has no effect on local stability.

This equation may be solved in terms of Greene's function,

$$G(x,\widehat{x},\omega)=\left[\overline{\phi}_+(x,\omega)\overline{\phi}_-(\widehat{x},\omega)H(x-\widehat{x})+\overline{\phi}_+(\widehat{x},\omega)\overline{\phi}_-(x,\omega)H(\widehat{x}-x)\right]/D(\omega)\ .$$

Here $\overline{\phi}_+$ and $\overline{\phi}_-$ are the solutions of the homogeneous equation vanishing at $+\infty$ and $-\infty$ respectively, and $H(x)$ is the Heaviside step function. $D(\omega)$ is the Wronskian of these solutions,

$$D(\omega) = \overline{\phi}'_+(x,\omega)\overline{\phi}_-(x,\omega) - \overline{\phi}_+(x,\omega)\overline{\phi}'_-(x,\omega) \ ,$$

where the prime indicates derivation with respect to x. The solution is

$$\overline{\phi}(x,\omega) = \int_{-\infty}^{\infty} d\widehat{x}\, G(x,\widehat{x},\omega)\Gamma(\widehat{x},\omega) \ ,$$

The response at time t is then

$$\widetilde{\phi}(x,t) = \frac{1}{2\pi}\int_{-\infty+ic}^{\infty+ic} d\omega e^{-i\omega t}\overline{\phi}(x,\omega) \ ,$$

where the Laplace inversion integral extends over the well-known Bromwich contour lying above all the singularities in the integrand.

III. PLANE-WAVE SOLUTIONS

Consider equilibria such that the plasma velocity-shear is everywhere directed along a constant magnetic field: $\mathbf{B} = B_0\widehat{\mathbf{z}}$ and $\mathbf{V} = V_z(x)\widehat{\mathbf{z}} + V_{y0}\widehat{\mathbf{y}}$. In such equilibria $k_\parallel$ and ω_d are constant, and plane-wave solutions of Eq. (1) may be obtained by Fourier transformation in the transverse (x) direction. The dispersion relation depends on the transverse and lateral components of the wavevector jointly through the constant $g_k = 1 + k_x^2 + k_y^2 = g_{ky} + k_x^2$. It is convenient to introduce the dimensionless wave parameters $K_\parallel =$

$k_\parallel c_s/(k_y \rho_s W_\parallel)$ and $\Omega_d = g_k \omega_d/\omega_*$. In terms of these parameters the dispersion relation is[9]

$$G(K_\parallel - 1)K_\parallel + \Omega_d - \Omega_d^2 = 0 \ ,$$

and the stability properties are determined by the single parameter $G = g_k(k_y \rho_s W_\parallel/\omega_*)^2$. The dispersion relation is a quadratic in the frequency Ω_d as well as the wavevector $K_\parallel$. Unstable roots will exist when its discriminant is negative,

$$1 + 4G(K_\parallel - 1)K_\parallel < 0 \ ,$$

or for parallel wavevectors lying in the range

$$[1 - (1 - 1/G)^{1/2}]/2 < K_\parallel < [1 + (1 - 1/G)^{1/2}]/2 \ .$$

For $G < 1$ the unstable range of $K_\parallel$ disappears. The stability condition is thus

$$(1 + k^2 \rho_s^2) \left(\frac{W_\parallel L_n}{c_s} \right)^2 < 1 \ .$$

Note that unstable waves always occur for sufficiently short wavelengths: this is characteristic of fluid models.

The unstable root of the eigenfrequency is

$$\Omega_d = \{1 + i[4G(1 - K_\parallel)K_\parallel - 1]^{1/2}\}/2 \ .$$

A plot of the dispersion relation is given in Fig. 1.

We calculate the maximum growth rate for later use: For fixed g_k, the growth is maximized by $K_\parallel = 1/2$, independently of the particular value of

g_k. The maximum is

$$\gamma = (g_k(k_y\rho_s W_\parallel/\omega_*)^2 - 1)^{1/2}\omega_*/2g_k \ .$$

This can in turn be maximized with respect to g_k at fixed k_y. The maximum lies at $g_k = 2(c_s/L_n W_\parallel)^2$. For $(L_n W_\parallel/c_s)^2 > 2$, however, this corresponds to an unphysical imaginary wavenumber: the maximum growth rate is then reached for $k = 0$.

In summary, for $(L_n W_\parallel/c_s)^2 > 1$ the long wavelengths become unstable but the growth rate maximum remains at finite wavelength. For $(L_n W_\parallel/c_s)^2 > 2^{1/2}$, $k = k_y$ becomes the most unstable wavenumber.

IV. PHASE-INTEGRAL SOLUTIONS

In the case of systems with weak shear, $s \sim w_\perp \ll 1$, the dielectric permittivity for oscillations with finite frequency ($\omega = \mathcal{O}(s^0)$) varies slowly on the scale of a wavelength. In this case solutions may be obtained by the phase-integral or WKB method. Equation (4) may be cast in canonical form with the change of independent variable $\xi = sx$:

$$\frac{d^2\overline{\phi}}{d\xi^2} + s^{-2}q(\xi,\omega)\overline{\phi} = 0 \ , \tag{4}$$

where

$$q(\xi,\omega) = -g_{ky} + \frac{1}{\omega_d} - w_\parallel\frac{\xi}{\omega_d^2} + \frac{\xi^2}{\omega_d^2}$$

and $\omega_d = \omega - w_\perp\xi/s$. The WKB approximation consists of retaining only the two lowest order terms in the expansion of the solution as an asymptotic

series in powers of s. A set of elementary solutions is

$$\overline{\phi}_{\pm}(\xi,\omega) = k_x^{-1/2} \exp\left[\pm i s^{-1} \int_{\xi_0}^{\xi} k_x \, d\xi\right] (1 + \mathcal{O}(s^2)) \; . \tag{5}$$

Here ξ_0 is an arbitrary reference point. The integrand $k_x = [q(\xi,\omega)]^{1/2}$ is interpreted as the local value of the transverse wavenumber. Note that the variation in the amplitude of the perturbation is determined primarily by the imaginary part of the phase integral $S_i = \mathrm{Im}[S(\xi,\omega)]$, where

$$S(\xi,\omega) = \int_{\xi_0}^{\xi} k_x(\widehat{\xi},\omega) \, d\widehat{\xi} \; .$$

It follows from the precise form of the error estimate in Eq. (5) that the WKB approximation applies *only* along paths such that the amplitude of the signal *does not decrease exponentially.* For the ϕ_+ solution in (5), for example, it is necessary that $dS_i/d\xi < 0$ or $\mathrm{Im}(k_x d\xi) < 0$. As a result, particular WKB solutions apply only in restricted sectors of the complex plane. The object of the phase integral method is to connect such solutions in order to obtain a global solution valid on the entire real line. The most complete description of this method may be found in a monograph by Heading.[12] We summarize the basic principles here.

The difficulty in extending the solution given by Eq. (5) is caused by the occurrence of *turning-points*, where $q(\xi,\omega) = 0$. Near turning points, the WKB approximation is *locally* invalidated. The true significance of turning points, however, lies in their influence on the *global* structure of the solution:[13] First, they are bifurcation points for the level contours of S_i in the complex

ξ-plane. Second, they give rise to branch cuts in the argument of the phase integral.

The global structure of the phase integral can be visualized with a Polya plot of the $k_x(x,\omega)$ function.[13] In this plot a complex function is represented by a field of vectors on a lattice of points corresponding to complex values of its argument. These vectors are directed at an angle equal to the phase of the function, and are given an amplitude proportional to the logarithm of its modulus. The Polya vectors for $k_x^*(\xi_r,\xi_i)$ are everywhere tangent to the lines of constant S_i and pointed in the direction of increasing S_r. Examples of Polya plots will be given below.

The level contours of S_i through the turning points, called anti-Stokes lines, play an important role in the theory. At a simple turning point ($|q_\xi| > 0$ where $q_\xi = (\partial q/\partial\xi)|_{\xi_0}$) one finds three anti-Stokes lines radiating outwards in directions given by the roots of $S_i = 0$, or $(z-z_0)^{-3} = q_\xi/|q_\xi|$. Since a monotonically nondecreasing path can only cross the anti-Stokes lines once, these lines are seen to constitute boundaries for the region of validity of the elementary WKB solutions. Extending the solution further necessitates crossing the branch cut. It must be emphasized that the branch cuts emanating from poles correspond to an actual discontinuity of the solution, while those emanating from turning points are only an artifact of the WKB approximation.

The principal features of Eq. (3) from the point of view of the WKB

analysis are as follows: It has two turning points, given by the roots of the quadratic equation

$$\omega(g_{ky}\omega - 1) + (sw_{\parallel} + w_{\perp} - 2g_{ky}\omega w_{\perp})\xi - (s^2 - g_{ky}w_{\perp}^2)\xi^2 = 0 \qquad (6)$$

and a double pole at $\xi = s\omega/w_{\perp}$. Near the double pole $k_x \sim q_p/(x - x_p)$, where q_p is a complex constant. Using $(x - x_p)^{-1} = (x - x_p)^*/|x - x_p|^2$, we see that the Polya vectors lie at fixed angle to the lines radiating from the pole, so that the pole will appear as a spiral sink. At large distances, the squared local transverse wavevector has the asymptotic behavior

$$k_x^2 \sim w_{\perp}^{-2}(s^2 - g_{ky}w_{\perp}^2) + sw_{\perp}^{-3}(w_{\perp}^2 + sw_{\parallel}w_{\perp} - 2\omega s^2)\xi^{-1} + \mathcal{O}(\xi^{-2}) \ . \qquad (7)$$

so that anti-stokes lines will logarithmically drift away from the real axis for $s^2 - g_{ky}w_{\perp}^2 > 0$, and from the imaginary axis otherwise.

V. EIGENMODES

Unstable eigenmodes occur when the Wronskian has a zero in the upper complex ω plane: such zeros indicate that the solution vanishing as $\xi \to -\infty$ is proportional to that vanishing as $\xi \to \infty$, or that there exits a globally well-behaved solution. Exact eigenmodes of Eq. (3) were given in Ref. 5 for arbitrary values of the shear, but it is instructive to see how this result can be recovered with the phase integral method in the limit of weak shear. This helps to understand the physical nature of the eigenmode stabilization

mechanism, as well as the difference between the eigenmode and convective instabilities.

It is necessary for the existence of eigenmodes that the frequency satisfy the generalized Bohr-Sommerfeld quantization condition:

$$s^{-1}\int_{\xi_1(\omega)}^{\xi_2(\omega)} k_x(\xi,\omega)\,d\xi = \pi(l+1/2)\ , \tag{8}$$

where $\xi_1(\omega)$ and $\xi_2(\omega)$ are the turning points in the complex plane and where the radial mode-number l ($l = 0, 1, 2...$) represents the number of nodes in the solution. This condition is insufficient, however, to demonstrate the existence of an eigenmode. The Bohr-Sommerfeld condition merely asserts the existence of two disconnected sectors in the complex plane where the solution is well behaved, or subdominant. Only if the limit points of the real line are shared among these two disconnected sectors will the solution be an acceptable eigenmode. In subsection A, we solve the Bohr Sommerfeld quantization condition perturbatively for small transverse mode-number. The asymptotic behavior of the resulting solutions is then examined in subsection B.

A. Bohr-Sommerfeld quantization

The radial mode-number l clearly plays a role similar to that of the transverse wavenumber k_x in the homogeneous case. By analogy one expects the most rapidly growing modes to correspond to moderate mode numbers $l \sim 1$. For general ω, however, the turning points are separated by a distance of order unity, so that the phase integral in Eq. (8) will be $\mathcal{O}(1/s)$. The lowest-

order modes are thus seen to correspond to values of the frequency such that the two turning points merge to lowest order:

$$q(\xi, \omega) = 0 \; ; \tag{9}$$

$$\frac{dq(\xi, \omega)}{d\xi} = 0 \; . \tag{10}$$

For the DKH instability, Eqs. (9)–(10) describe the double roots of Eq. (6).

Equation (10) is applied to Eq. (6) to evaluate the position of the double turning point ξ_{2tp}:

$$\xi_{2tp} = \frac{s w_\parallel + w_\perp (1 - 2 g_{ky} \omega)}{2(s^2 - g_{ky} w_\perp^2)} \; .$$

Eliminating ξ_{2tp} from Eqs. (9) and (6) yields the dispersion relation

$$(s w_\parallel + w_\perp - 2 g_{ky} \omega w_\perp)^2 - 4(g_{ky} w_\perp^2 - s^2)(g_{ky} \omega - 1)\omega = 0 \; .$$

This may be solved for the lowest-order approximation to the Bohr-Sommerfeld frequency,

$$\omega_0 = \frac{s + w_\parallel w_\perp g_{ky} \pm [(1 - g_{ky} w_\parallel^2)(s^2 - g_{ky} w_\perp^2)]^{1/2}}{2 s g_{ky}} \; .$$

Instability follows when the discriminant $(1 - g_{ky} w_\parallel^2)(s^2 - g_{ky} w_\perp^2)$ is negative. The $(w_\perp, w_\parallel)$ plane may thus be separated into four regions bounded by the lines $1 = g_{ky} w_\parallel^2$ and $s^2 = g_{ky} w_\perp^2$, as shown in Fig. 2. A robust (i.e. $\gamma = \mathcal{O}(s^0)$) growth rate is found in regions 2 and 4. In order to ascertain the stability of regions 1 and 3, where the approximate Bohr-Sommerfeld frequency is real, it is necessary to calculate the next order correction. The first terms in the

expansion of the function $q(\xi,\omega)$ as a Taylor series in powers of $\xi - \xi_{2tp}$ and $\omega - \omega_0$ are

$$q(\xi,\omega) = q_{\xi\xi}(\xi - \xi_{2tp})^2/2 + q_\omega(\omega - \omega_0) + \dots ,$$

where $q_\omega = \partial q(\xi,\omega)/\partial\omega|_{\omega_0,\xi_{2tp}}$ and $q_{\xi\xi} = \partial^2 q(\xi,\omega)/\partial\xi^2|_{\omega_0,\xi_{2tp}}$. Using this expansion in the dispersion relation, one finds

$$\omega = \omega_0 + (l+1/2)s(-2q_{\xi\xi})^{1/2}/q_\omega \ . \tag{11}$$

We calculate

$$\frac{q_{\xi\xi}}{2} = \frac{1 - g_{ky}w_\perp^2/s^2}{\omega_{d2tp}^2} \ ;$$

$$q_\omega = \frac{s(1 - g_{ky}w_\parallel^2)^{1/2}}{\omega_{d2tp}^2(s^2 - g_{ky}w_\perp^2)^{1/2}} \ ,$$

where $\omega_{d2tp} = \omega_0 - w_\perp\xi_{2tp}/s$. Substitution into (11) yields

$$\omega - \omega_0 = \pm i(s^2 - g_{ky}w_\perp^2)^{1/2}[s \pm (s^2 - g_{ky}w_\perp^2)^{1/2}(1 - g_{ky}w_\parallel)^{-1/2}]/(2sg) \ .$$

It follows that the Bohr-Sommerfeld condition has weakly unstable roots ($\gamma \sim s$) in region 1 (i.e. for $s^2 - g_{ky}w_\perp^2 > 0$ and $1 - g_{ky}w_\parallel^2 < 0$), but that region 3 is stable. The contour lines for the imaginary part of the frequency are shown in Fig. 2.

B. Boundary conditions

The roots of the Bohr-Sommerfeld condition will correspond to eigenmodes if the associated WKB solutions are well-behaved at $\pm\infty$. In order

to determine whether the subdominant root at $-\infty$ is properly connected to the subdominant root at $+\infty$, we apply the Nyquist theorem to a closed contour consisting of the real axis and a semi-circle surrounding the lower half complex plane. In order to avoid having to discuss separately the case when the real axis lies between the turning points supporting the standing-wave structure, the contour is deformed so as to leave these turning points on the same side. By the Nyquist theorem, the image of this contour under the map $k_x^2 = q(\xi, \omega)$ will circle the origin a number of times equal to the number of zeros of $q(\xi, \omega)$ in the lower half of the ξ plane. Since this number is even, we conclude that the real line connects together the same roots of k_x at $\pm\infty$. Note that for any particular set of parameters, the connectivity of the roots can be determined by inspection of the Stokes diagram. The Nyquist analysis is necessary, however, to prove general results.

To determine if a solution connecting the same roots of k_x at $\pm\infty$ corresponds to a well-behaved mode, consider the asymptotic expansion for the potential, Eq. (7). There is a critical value of the velocity shear, $w_\perp = s g_{ky}^{-1/2}$, such that k_x vanishes at infinity. We consider the cases of subcritical and supercritical velocity shear separately.

Subcritical velocity shear:

For $w_\perp < s g_{ky}^{-1/2}$, k_x is real to lowest order. The imaginary part of k_x is determined by the next order term, and changes sign with ξ. The Bohr-

Sommerfeld solutions will thus be well-behaved. The Stokes plot for this case is shown in Fig. 3(a): The real axis is seen to connect two disconnected Stokes sectors. The imaginary part of the phase integral in Fig. 3(b), shows the decay of the amplitude in both directions.

Supercritical velocity shear:

For $w_\perp > s g_{ky}^{-1/2}$, k_x is imaginary and keeps the same sign as $\xi \to \pm\infty$. The Bohr-Sommerfeld solutions will thus be divergent. The Stokes plot for this case is shown in Fig. 4(a): The real axis is seen to connect two adjacent Stokes sectors. The behavior of the phase integral is shown in Fig. 4(b), showing divergence for $x \to +\infty$.

In summary, unstable eigenmodes are found only for $w_\perp < s g_{ky}^{-1/2}$, in regions 1 and 2. In region 2, the eigenmodes are robustly unstable: in region 1 they are only weakly unstable. No unstable eigenmodes are found for $w_\perp > s g_{ky}^{-1/2}$, independently of the strength of the parallel component of velocity shear (regions 3 and 4).

VI. WAVE AMPLIFICATION

Initial perturbations may be amplified even in the absence of unstable eigenmodes. The investigation of the initial-value problem is greatly facilitated by the existence of an analytic expression for the phase-integral. Taking

care not to introduce spurious branch cuts, we find

$$S(\xi;\omega) = \left(\frac{s^2}{w_\perp^2} - g_{ky}\right)^{1/2} \left\{ (\delta\xi_1)^{1/2}(\delta\xi_2)^{1/2} - (\xi_1+\xi_2)\ln[(\delta\xi_1)^{1/2} + (\delta\xi_2)^{1/2}] \right.$$

$$\left. + \xi_1^{1/2}\xi_2^{1/2} \ln\left[\frac{\xi_2^{1/2}(\delta\xi_1)^{1/2} + \xi_1^{1/2}(\delta\xi_2)^{1/2}}{\xi_2^{1/2}(\delta\xi_1)^{1/2} - \xi_1^{1/2}(\delta\xi_2)^{1/2}}\right] \right\}$$

where $\delta\xi_1 = \xi - \xi_1$ and $\delta\xi_2 = \xi - \xi_2$.

Two problems will be treated: The steady-state monochromatic point-source, and the propagation of a localized initial perturbation.

A. Steady-state point source

The response to a steady-state monochromatic point-source, or antenna, is most easily evaluated: it is given directly by Greene's function. By steady state, it is meant here that the driving frequency has fixed real and imaginary parts, or that the amplitude of the source increases at a constant rate.

It is apparent from the exponential form of the WKB solutions that extrema in the imaginary part of the phase integral will give rise to Gaussian peaks of width $s^{1/2}$ in the response. These peaks occur when $S_i'(\xi) = \mathrm{Im}[k_x(\xi)]$ vanishes for some real ξ. That is, they correspond to roots of the local dispersion relation for real ξ and k_x. These peaks may appear to be eigenmodes in numerical investigations using shooting codes: frequency convergence studies are then necessary to discriminate between wave resonances and eigenmodes.

We consider three cases: The first corresponds to the critical velocity shear for eigenmode stabilization, the second satisfies the condition for confluence of the turning points, and the third corresponds to vanishing perpendicular component of the velocity-shear.

1. **Critical Velocity Shear**

   For resonant velocity shear ($w_\perp^{-2} g_{ky} = s^2$) one of the turning points is removed to infinity, and the WKB structure is determined by the remaining turning point and the double pole (Fig. 5(a)). Geometrically, the local instability appears as the point where the lines of constant S_i are tangent to the real axis, corresponding to an extremum of S_i. To fix ideas, let the antenna be placed to the right of the extremum. The signal amplitude must decay for $x \sim \pm\infty$. Consider the appropriate WKB integral from $-\infty$ towards the antenna. The amplitude, given approximately by $\exp(-S_i)$, is found to increase up to the point of local instability (Fig. 5(b)). Beyond this point, $-S_i$ decreases. The real axis is no longer a good path of integration for the WKB method, but it remains possible, by deforming the path of integration, to reach points beyond the extrema with paths of nondecreasing $-S_i$.

   On the right of the second anti-Stokes line, however, the WKB paths must circle above the turning point and cross the branch-cut. This changes the sign of the root of k_x. Consequently, the signal amplitude

increases towards the antenna on the right side of the second anti-Stokes line.

The maximum amplification, for a given driving frequency, is thus attained when the antenna is placed at the intersection of the anti-Stokes line with the real axis: It is given by the exponential of the path integral from the turning point (the vertex of the three anti-Stokes lines) to the point of local instability (where the Polya vector is parallel to the real axis). Note that the amplification from the turning point to the point of local instability is the same as that from the intersection of the anti-Stokes line with the real axis to the point of local instability, since an anti-Stokes line connects both starting points.

It is clear from the form of the eikonal that the maximum amplification will increase without bound as the value of k_x at the resonance point is increased, since this has the effect of moving the turning-point away from the real axis. This is a defect of the fluid model. To obtain meaningful bounds on the amplification, we fix $k_x\rho_s = 1$ and optimize the driving frequency by varying the transverse position x of the resonance point (or equivalently $k_\parallel$). Fig 5 shows the Stokes diagram and phase integral for the most amplified frequency.

2. **Confluent Turning-Points:**

Confluence has the effect of increasing the gradient of the eikonal at

moderate distances from the turning-points. This leads to greater amplification. The proximity of the pole has a similar effect. The result is that this case corresponds to the maximum amplification (for fixed k_x) as a function of $w_\perp$ (Fig. 6).

3. **Vanishing Perpendicular Velocity-Shear:**

   We last consider the case of purely parallel velocity shear, $w_\perp = 0$. Here, the double pole is infinitely removed from the unstable region and S_i has two extrema on the real axis. If one corresponds to a maximum for the signal amplitude, the other must correspond to a minimum. The largest possible amplification will be the lesser of two numbers: The amplification between the turning point and the point of local instability, and the amplification between the point of local instability and the secondary extremum. The proximity of two turning points and a nearby minimum results in weak variation of the eikonal S, and thus in weak amplification. The gradient of S is further weakened, for vanishing perpendicular velocity-shear, by the absence of the Doppler resonance (i.e. the double pole).

The three cases described above correspond to the numbered points in Fig. 6, where the variation of the maximum amplification is shown as a function of the perpendicular velocity-shear for $k_x\rho_s = 1$. The largest amplification is obtained for $w_\perp = .04$, corresponding to the case where the

turning-points have merged. For larger values of the velocity shear, the amplification decreases slowly, as the inverse power of the shear.

The maximum amplification is reminiscent of the scattering-state resonances of quantum mechanics. Note that the maximum arises from the behavior of the phase integral. The eigenmodes, by contrast, correspond to the vanishing of the Wronskian in the denominator of Greene's function. Because of the analyticity of the scattering matrix, the scattering-states (travelling waves) feel the presence of nearby (linearly independent) eigenmodes. Of course, unstable eigenmodes will always dominate the evolution if they are excited in the initial state.

B. Wave-packet amplification

By virtue of the separation of scales between the density gradient length L_n and the shear length L_s, it is possible to construct wavepackets with well-defined position x_0 and wavelength k_0:

$$\tilde{\phi}(x,0) = \tilde{\phi}_0 \left(\frac{\sigma}{2\pi}\right)^{1/2} \exp\left[-\frac{\sigma}{2}(x-x_0)^2\right] e^{ik_0 x} \; .$$

For simplicity, we restrict the discussion to Bromwich paths such that $\mathrm{Im}(\omega) > \gamma_{\max}$, where $\gamma_{\max}$ is the largest local growth rate corresponding to $k_x = 0$. This ensures that the turning-points will not cross the real x-axis during the inverse Laplace transform. The generalization to $0 < \mathrm{Im}(\omega) < \gamma_{\max}$ is straightforward; all that is required is to change the sign of k_x upon crossing an anti-Stokes line.

For $x > x_0$, the Laplace transform of the response is given by

$$\overline{\phi}(x,\omega) = \left(\frac{\sigma}{2\pi}\right)^{1/2} \phi_0 \int_{-\infty}^{\infty} d\hat{x}\, \Lambda(sx, s\hat{x}, \omega) \exp\left(\frac{i}{s}\int_{sx_<}^{sx_>} k_x(\xi,\omega)d\xi + ik_0\hat{x} - \sigma(\hat{x}-x_0)^2/2\right) ,$$

where $x_<$ ($x_>$) is the lesser (greater) of x and $\hat{x}$, and Λ is a slowly varying coefficient:

$$\Lambda(sx, s\hat{x}, \omega) = \frac{1}{2}\, g_{k0}[k_x(sx,\omega)k_x(s\hat{x},\omega)]^{-1/2}\hat{\omega}_d^{-1} .$$

Here $\hat{\omega}_d = \omega - w_\perp \hat{x}$ and $g_{k0} = g_{ky} + k_0^2$.

The spatial integral may be evaluated by the method of steepest descent. The saddle point $\hat{x}$ is determined by

$$k_0 - k_x(s\hat{x},\omega) + i\sigma(\hat{x}-x_0) = 0 .$$

For $\sigma \sim 1$, one has $\hat{x} - x_0 \sim 1$ and $k_x(s\hat{x},\omega) = k_x(sx_0,\omega) + \mathcal{O}(s)$. It follows

$$\overline{\phi}(x,\omega) = -\phi_0 \Lambda(sx, sx_0, \omega) \exp\left(\frac{i}{s}\int_{sx_0}^{sx} k_x(\xi,\omega)d\xi + ik_0x_0 - \frac{1}{2\sigma}\left(k_x(sx_0,\omega) - k_0\right)^2\right) ,$$

Note that the spatial Fourier transform of the initial wavepacket is

$$\tilde{\phi}(k,0) = \tilde{\phi}_0 \exp\left[-\frac{1}{2\sigma}(k-k_0)^2\right] e^{i(k_0-k)x_0} .$$

The Laplace transform of the response may thus be interpreted as the product of the Fourier amplitude of the wavevector $k_x(sx_0,\omega)$ in the initial state with the steady-state amplification for the frequency ω. The latter term dominates for frequencies such that the local wavevector approximately matches the initial wavevector $k_x(sx_0,\omega) - k_0 \sim 1$.

The Laplace inversion integral is

$$\tilde{\phi}(x,t) = \frac{\phi_0}{2\pi}\int_{-\infty+ic}^{\infty+ic} d\omega\Lambda(sx, sx_0, \omega)\exp[\mathcal{L}(sx, sx_0, \omega t)] \ ,$$

where

$$\mathcal{L}(sx, sx_0, \omega t) = i\left(\frac{1}{s}\int_{sx_0}^{sx} k_x(\xi,\omega)d\xi + k_0x_0 - \omega t\right) - \frac{1}{2\sigma}\left(k_x(sx_0,\omega) - k_0\right)^2 \ .$$

The function $\mathcal{L}$ bears deceptive resemblance to a classical action, but it must be remembered that the phase integral is to be carried-out at constant ω. As we shall presently show, the dominant frequency is not conserved during the evolution of a wavepacket in an inhomogeneous active medium.

The inversion integral may be carried out by the method of stationary phase. It is dominated by the contribution from the frequency ω_0 such that $\partial\mathcal{L}/\partial\omega = 0$, or

$$t = \frac{1}{s}\int_{sx_o}^{sx}\left(\frac{\partial k_x}{\partial\omega}\right)_{\omega_0} d\xi \ , \tag{12}$$

where terms of $\mathcal{O}(1)$ associated with the initial Fourier amplitude have been neglected. The stationary phase condition, Eq. (12), must be solved for ω_0, given the time and position of observation. The integral in Eq. (12) clearly represents the time taken by a wavepacket of complex frequency $\omega_0 = \omega_{0r} + i\gamma$ to travel from the initial position x_0 to the observation point x at the group velocity $v_g = \partial\omega/\partial k_x$. The stationary phase approximation to the integral is then

$$\tilde{\phi}(x,t) = -\phi_0\left(\frac{i}{\pi}\int_{sx_0}^{sx}\frac{\partial^2 k_x}{\partial\omega^2}\,d\xi\right)_{\omega_0}^{-1/2}\Lambda(sx, sx_0, \omega_0)\exp[\mathcal{L}(sx, sx_0, \omega_0)] + \mathcal{O}(s) \ ,$$

where ω_0 is determined by Eq. (12). The amplification is found to be increased over the imaginary part of the phase integral S_i by the growth rate factor $\exp(\gamma t)$, where $\gamma = \mathrm{Im}(\omega_0)$. This may be understood by recalling that the steady-state amplification compares the amplitude of the signal *being emitted* at time t to the amplitude of the signal which *was emitted* at time $t' = t - \int dx/v_g$.

In practice Eq. (12) is difficult to solve and it is more convenient to specify the frequency ω_0 and to use Eq. (12) to determine x, x_0 and t. The frequency ω_0 is itself specified in terms of the local dispersion relation by choosing k_{x0} and $k_{\|0} = k_y x_0/L_s$. For fixed k_{x0}, the maximum amplification is generally obtained in the middle of the unstable region, for $sx_0 = w_\|/2$. Adopting this value for sx_0, the dependence of the maximum convective amplification on the perpendicular velocity shear is shown in Fig. 7 for $k_{x0} = 0$ and $k_{x0} = 1$. The qualitative dependence is similar to that for steady-state amplification but numerically much larger. This can be explained by the relative proximity of the turning point to the real axis for $k_x \sim 1$. This reduces the imaginary part of the wavevector responsible for steady-state amplification, while it enhances the convective amplification by reducing the group velocity in the unstable region.

VII. DISCUSSION

We have shown that the amplification of a localized initial perturbation remains large for velocity shears greater than the critical value for stabilization of the normal modes. The maximum amplification for a driven steady-state wave is shown in Fig. 6, and that for a launched wavepacket in Fig. 7. Note that these figures correspond to a magnetic shear $s = 0.1$. The amplification for different values of s is readily obtained by dividing the ordinate by $10\,s$.

Convective instabilities unfortunately fall outside the scope of classical quasilinear theory, so that it is difficult to draw conclusions as to their nonlinear behavior even in the simplest context. The effect of convective instabilities on the fluctuation level in thermal equilibrium has been considered by Kent and Taylor.[8] The dressed test-particle model used by these authors, however, restricts consideration to steady-state perturbations with real frequency. We have found in this study that wavepackets with positive growth rates are much more strongly amplified.

The effect of rotation shear on the stability of drift-acoustic waves is of interest in connection with the problem of transport in tokamaks injected with neutral beams. It was suggested in Ref. 5 that a regime of improved confinement could be attained by increasing the value of the toroidal rotation shear. Sheared toroidal rotation results in a small but significant perpendicular component of flow-shear. As a result of the absolute nature of the

eigenmode stabilization criterion, $(dV/dr)_\perp = c_s/L_s$, the normally destabilizing property of the parallel component of the flow-shear is ineffective for supercritical velocity-shear.

The present work shows that *convective* instabilities, by contrast, are *destabilized* by moderate values of the perpendicular rotation shear. These instabilities can never be completely stabilized, although the amplification factor decreases as the shear is increased beyond the resonant value $(d\mathbf{V}/dx)_\perp = c_s/L_s$. Note that the velocity shear in the edge layer of H-mode discharges is typically several times the resonant value, so that convective instabilities are not likely to be severe in this region. For the levels of rotation shear attained in the core, however, purely toroidal rotation is convectively destabilizing.

Experimentally, it is observed that tangential neutral-beam injection does not significantly modify the transport properties. A possible explanation for this is that the eigenmode stabilization effect is offset by the convective mode destabilization. Another possibility is that the destabilizing parallel rotation shear results in the generation of stabilizing poloidal flows through the Reynolds stress.[14] In either case, the present work implies that driving poloidal flows directly through perpendicular neutral beam injection is more promising, as a method of suppressing microturbulence, than driving toroidal rotation.[15]

Acknowledgments

It is a pleasure to acknowledge helpful discussions with H.L. Berk and J.B. Taylor. We would also like to thank R.B. White for use of his WKB code. This work was supported by the U.S. Department of Energy contract No. DE-FG05-80ET-53088 .

Appendix A: THE BOHR-SOMMERFELD QUANTIZATION CONDITION

To demonstrate the Bohr-Sommerfeld quantization condition we begin by showing that every solution is ill-behaved unless the phase integral separating the turning-points is real.

It is useful to distinguish the WKB *functions*, defined over the entire complex plane by

$$f_{\pm}(\xi) = k_x^{-1/2} \exp\left[\pm i s^{-1} \int_{\xi_0}^{\xi} k_x \, d\xi\right] ,$$

from the actual *solutions*. The WKB functions are of course locally proportional to the solutions, with different constants of proportionality in different sectors of the complex plane. Following Heading, we use the notation

$$f_+(\xi, \omega) = (\xi_0, \xi) \ ;$$

$$f_-(\xi, \omega) = (\xi, \xi_0) \ ,$$

so that we may choose locally

$$\overline{\phi}_+(\xi, \omega) = (\xi_0, \xi) \ ;$$

$$\overline{\phi}_-(\xi, \omega) = (\xi, \xi_0) \ .$$

In any given sector bounded by anti-Stokes lines one of these solutions is exponentially large and the other exponentially small: they are called the

dominant and subdominant solutions respectively. Continuation of the solutions across the branch-cut in the counterclockwise sense is then given by

$$\overline{\phi}_+(\xi,\omega) = -i[\xi_0,\xi_t](\xi,\xi_t) \ ;$$

$$\overline{\phi}_-(\xi,\omega) = -i[\xi_t,\xi_0](\xi_t,\xi) \ ,$$

where ξ_t is the turning point and

$$[\xi_0,\xi_t] = \exp[is^{-1}S(\xi_t,\omega)] \ .$$

The above considerations allow a WKB solution to be extended throughout the complex plane with the exception of a narrow strip surrounding the anti-Stokes line behind the turning point. An elegant technique for describing the solution in the vicinity of this line has been given by Heading. This technique is used below to derive the Bohr-Sommerfeld quantization relation. If the phase-integral has an imaginary part, the sets of anti-Stokes lines corresponding to different turning points are distinct and non-intersecting, and every point in the complex plane may be reached without crossing an anti-Stokes line more than once (except for points near the anti-Stokes lines behind each turning point). In particular it is always possible to find a good path extending from $-\infty$ to $+\infty$ along which the solution diverges.

When the phase integral between the two turning points is purely real, by contrast, the anti-Stokes lines form a connected set dividing the complex plane into four sectors (Figs. 3–4). The first two are contiguous to every other sector. The other two are separated by the first two.

If either limit-point of the real line belongs to one of the contiguous sectors, the corresponding WKB solution will diverge in every neighboring sector and thus also at the other limit-point. If the limit-points lie in disconnected sectors, however, the solution cannot be represented by a single WKB function, since the integration path may only cross one anti-Stokes line. To determine if a well-behaved solution exists we must match the particular WKB solutions, using the property that any three solutions are linearly dependent. Let the well-behaved solutions in each disconnected wedge be $\phi_1(\xi) = (\xi_1, \xi)$ and $\phi_2(\xi) = (\xi_2, \xi)$, where ξ_1 and ξ_2 are the corresponding turning points.

These solutions may be expressed as linear combinations of the two elementary solutions defined with respect to reference points in the contiguous sectors. For this discussion it is convenient to extend the branch cut from one turning point to the other below the anti-Stokes line. On the anti-Stokes line joining the two turning points we have

$$\phi_1(\xi) = A(\xi_1, \xi) + B(\xi, \xi_1) \ . \tag{A1}$$

Just above the anti-Stokes line the first WKB solution is

$$\phi_1(\xi) = (\xi_1, \xi)$$

while just below the anti-Stokes line the WKB path must cross the branch cut in the positive sense so that the first solution is

$$\phi_1(\xi) = -i(\xi, \xi_1) \ .$$

Matching these results we find that on the connecting anti-Stokes line,

$$\phi_1(\xi) = (\xi_1, \xi) - i(\xi, \xi_1) \ . \tag{A2}$$

Likewise, we find for the second solution

$$\phi_2(\xi) = (\xi_2, \xi) + i(\xi, \xi_2) \ .$$

This may be factorized as

$$\phi_2(\xi) = [\xi_2, \xi_1](\xi_1, \xi) + i(\xi, \xi_1)[\xi_1, \xi_2] \ . \tag{A3}$$

Matching the first and second solutions yields the Bohr-Sommerfeld quantization rule,

$$[\xi_1, \xi_2] = i$$

or

$$s^{-1} \int_{\xi_1}^{\xi_2} k_x \, d\xi = \pi(l + 1/2) \ , \tag{A4}$$

For $l \sim 1$ the analysis used to derive Eq. (A4) is invalidated, as the WKB approximation does not hold between the turning points. An alternative treatment using Weber's equation, however, can be shown to lead to the same result.

REFERENCES

1. G. M. Staebler and R. R. Dominguez, Nucl. Fusion **31**, 1891 (1991).

2. S. Hamaguchi and W. Horton, Phys. Fluids B **4**, 319 (1992).

3. X.-H. Wang and P. H. Diamond, Phys. Fluids B **5**, 319 (1993).

4. A. B. Hassam, Comments Plasma Phys. Controlled Fusion **14**, 275 (1992).

5. F. L. Waelbroeck, T. M. Antonsen, Jr., P. N. Guzdar, and A.B. Hassam, Phys. Fluids B **4**, 2441 (1993).

6. S. Migliuolo and A. K. Sen, Phys. Fluids B **2**, 3047 (1990).

7. B. Coppi, G. Laval, R. Pellat and M. N. Rosenbluth, Nucl. Fusion **6**, 261 (1966).

8. A. Kent and J. B. Taylor, Phys. Fluids **12**, 209 (1969).

9. N. D'angelo, Phys. Fluids **8**, 1748 (1965).

10. P. J. Catto, M. N. Rosenbluth, and C. S. Liu, Phys. Fluids **16**, 1719 (1973).

11. D. Pearlstein and H. L. Berk, Phys. Rev. Lett. **23**, 220 (1969).

12. J. Heading, *An Introduction to Phase Integral Methods*, (Wiley and Sons, New York, 1962).

13. R. B. White, J. Comp. Phys. **31**, 409 (1979).

14. X. N. Su, P.N. Yushmanov, J. Q. Dong, and W. Horton, Phys. Plasmas **1**, 1905 (1995).

15. A. B. Hassam, T. M. Antonsen, Jr., J. F. Drake, P. N. Guzdar, C. S. Liu, D. R. McCarthy and F. L. Waelbroeck, Phys. Fluids B **5**, 2519 (1993).

FIGURE CAPTIONS

1. Local dispersion relation represented by the lines of constant g_k and $k_\parallel$ in the complex frequency plane. Here $w_\parallel = 2$.

2. Contour plot for the imaginary part of the Bohr-Sommerfeld frequency, γ, for $g_{ky} = 2$. The lines of constant γ are spaced by $0.1\omega_*$ The four numbered regions are bounded by the thick lines $w_\perp = s g_{ky}^{-1/2}$ and $w_\parallel = g_{ky}^{-1/2}$. Only regions 1 and 2 have well-behaved unstable eigenmodes.

3. (a) Stokes diagram of the DKH eigenmode for subcritical velocity shear. The parameters are $s = 0.1$, $g_{ky} = 2$, $w_\parallel = 2$, and $w_\perp = 0.04$ (corresponding to a point in region 2 of Fig. 2). (b) Real part of the phase integral along the real x-axis, in dB: $A(x) = 10 \log_{10} |\phi(x)/\phi_0|$.

4. (a) Stokes diagram for the Bohr-Sommerfeld frequency with supercritical velocity shear. The parameters are $s = 0.1$, $g_{ky} = 2$, $w_\parallel = 0.5$, and $w_\perp = 0.1$ (corresponding to a point in region 4 of Fig. 2). (b) Real part of the phase integral along the real axis.

5. (a) Stokes diagram of a convective instability in a plasma with critical velocity shear. The parameters are the same as in Fig. 3 except for $\omega/\omega_* = 0.91 + i0.53$, corresponding to $k_x \rho_s = 1$, $k_\parallel c_s/\omega_* = 1.242$. (b) Real part of the phase integral along the real axis for the left WKB solution, $A(x) = 10 \log_{10} |\phi_-(sx, \omega)/\phi_0|$.

6. Maximum steady-state amplification, $A_{\max} = 10 \log_{10} |\phi_{\max}/\phi_0|$, as a function of the perpendicular component of the velocity shear for $k_x \rho_s = 1$, $s = 0.1, g_{ky} = 2$, and $w_{\|} = 2$. The numbered points correspond to the cases discussed in the text. The continuous line is an interpolation.

7. Maximum convective wavepacket amplification as a function of the perpendicular component of the velocity shear for the parameters of Fig. 6.

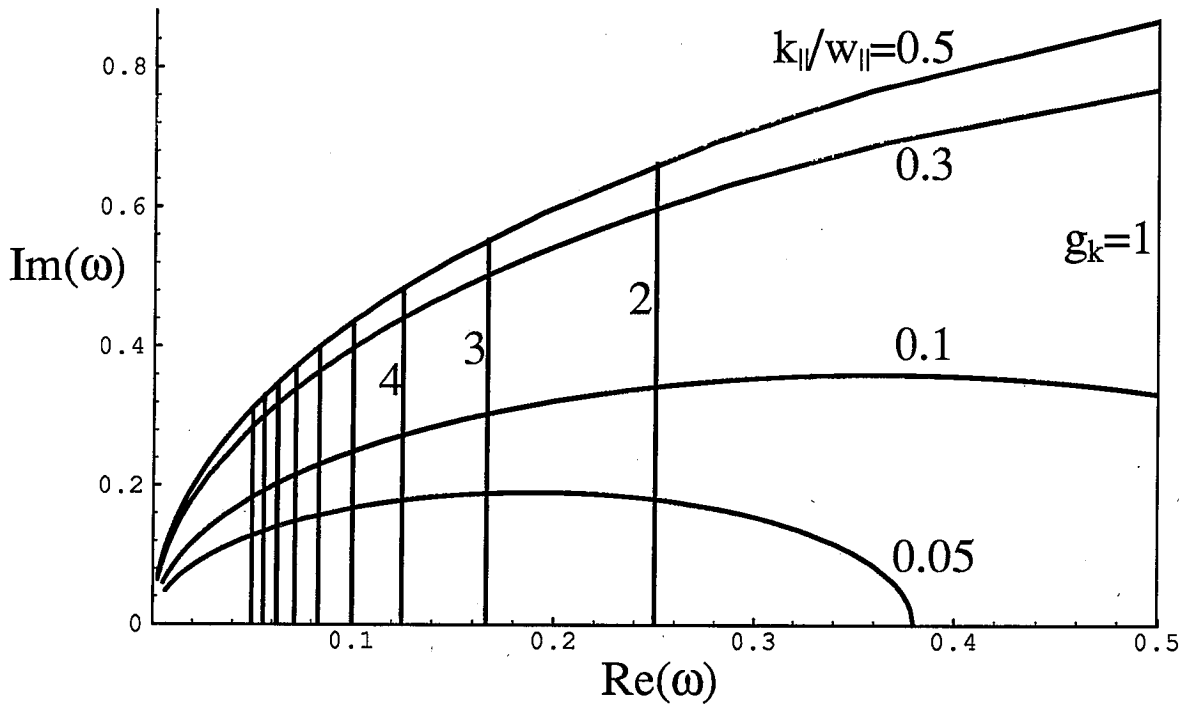

Fig. 1

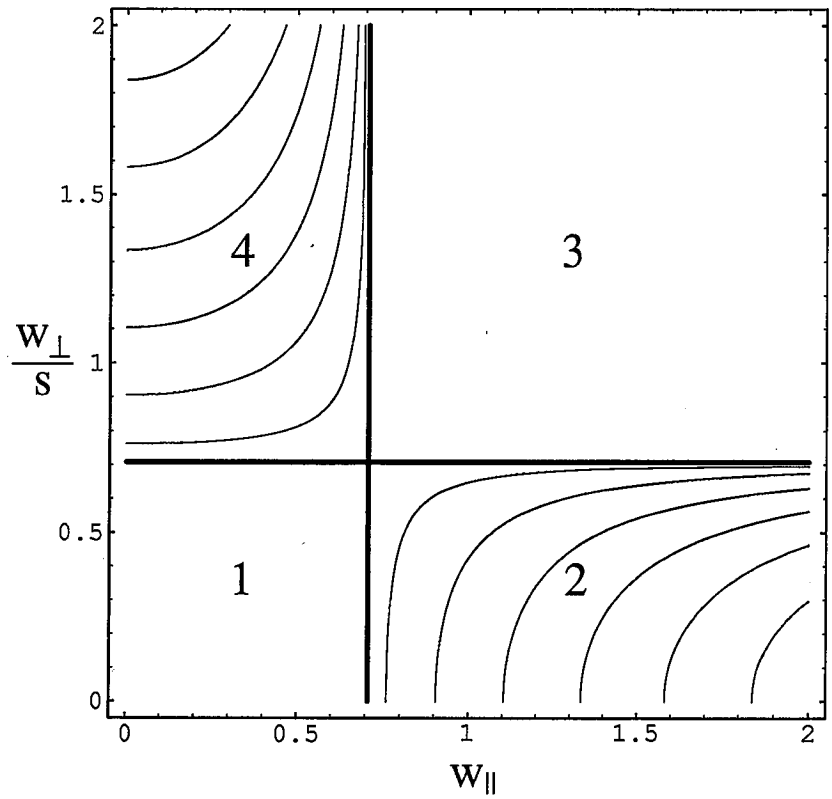

Fig. 2

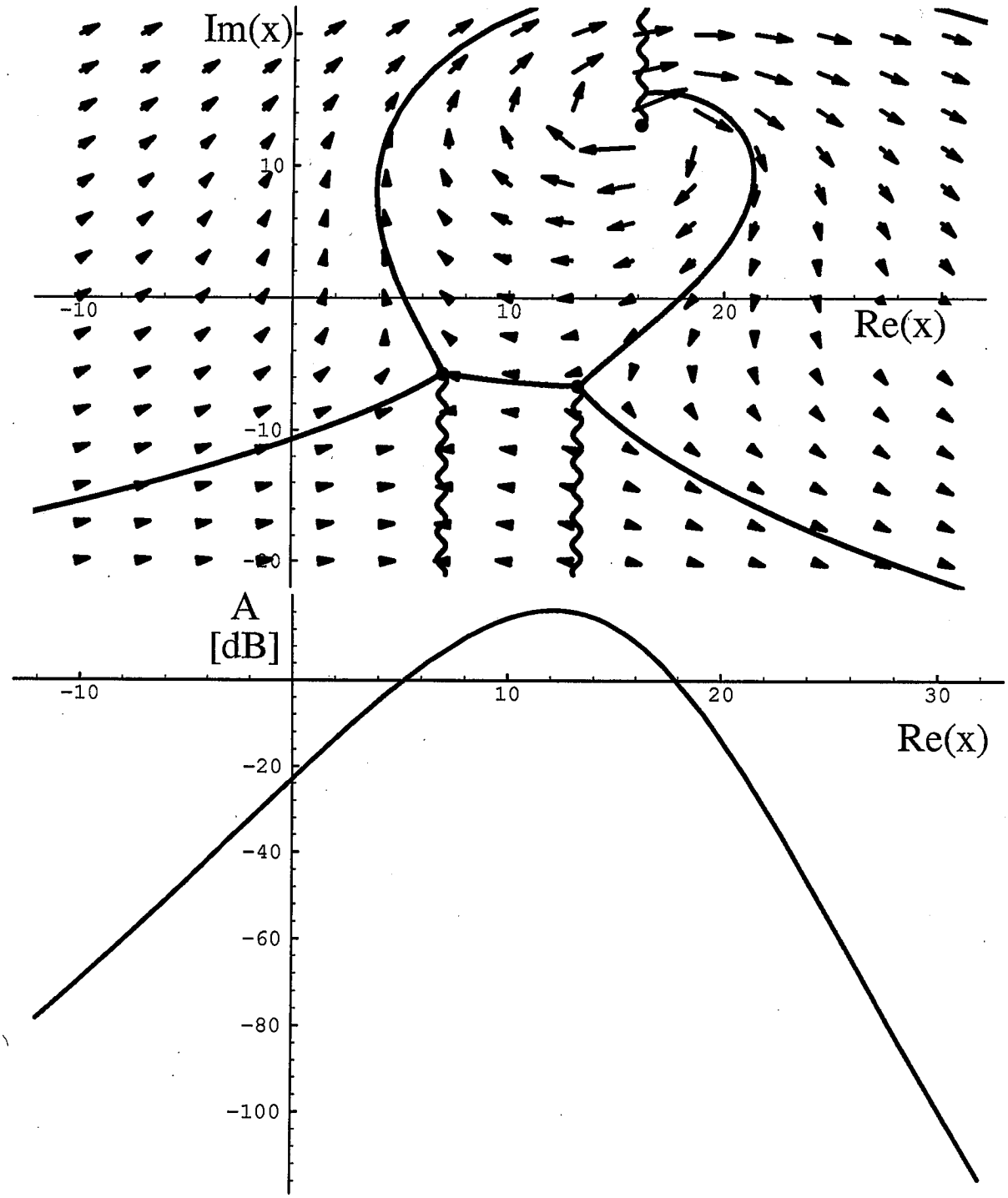

Fig. 3

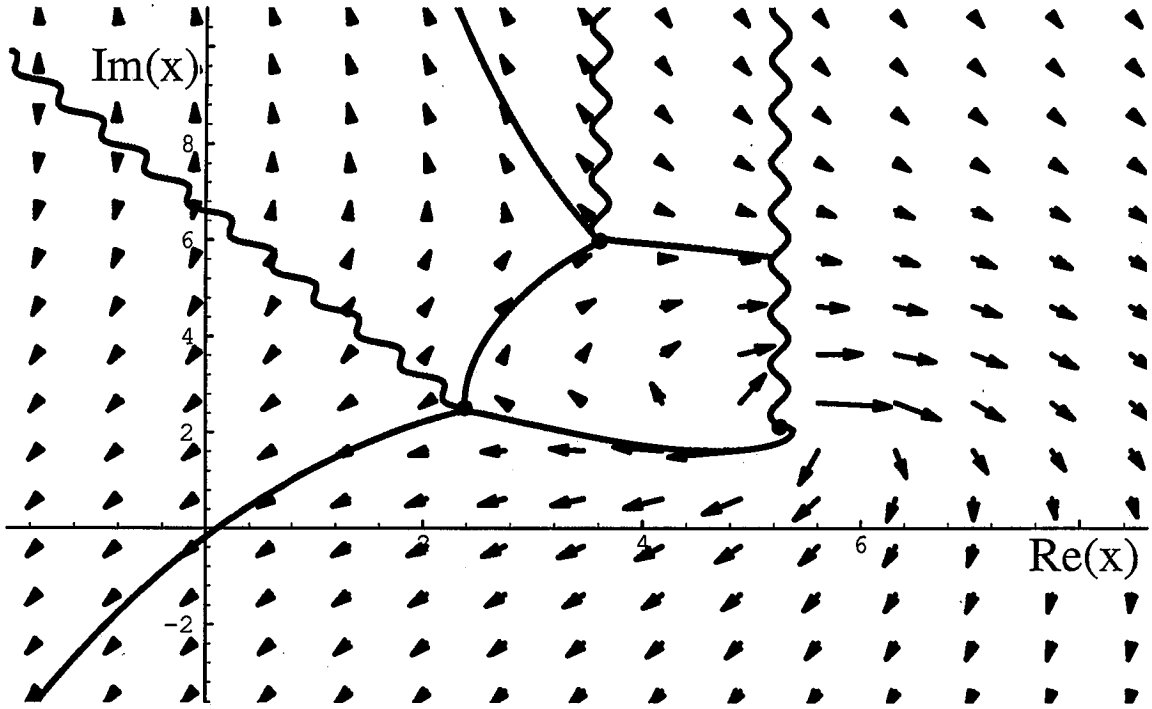

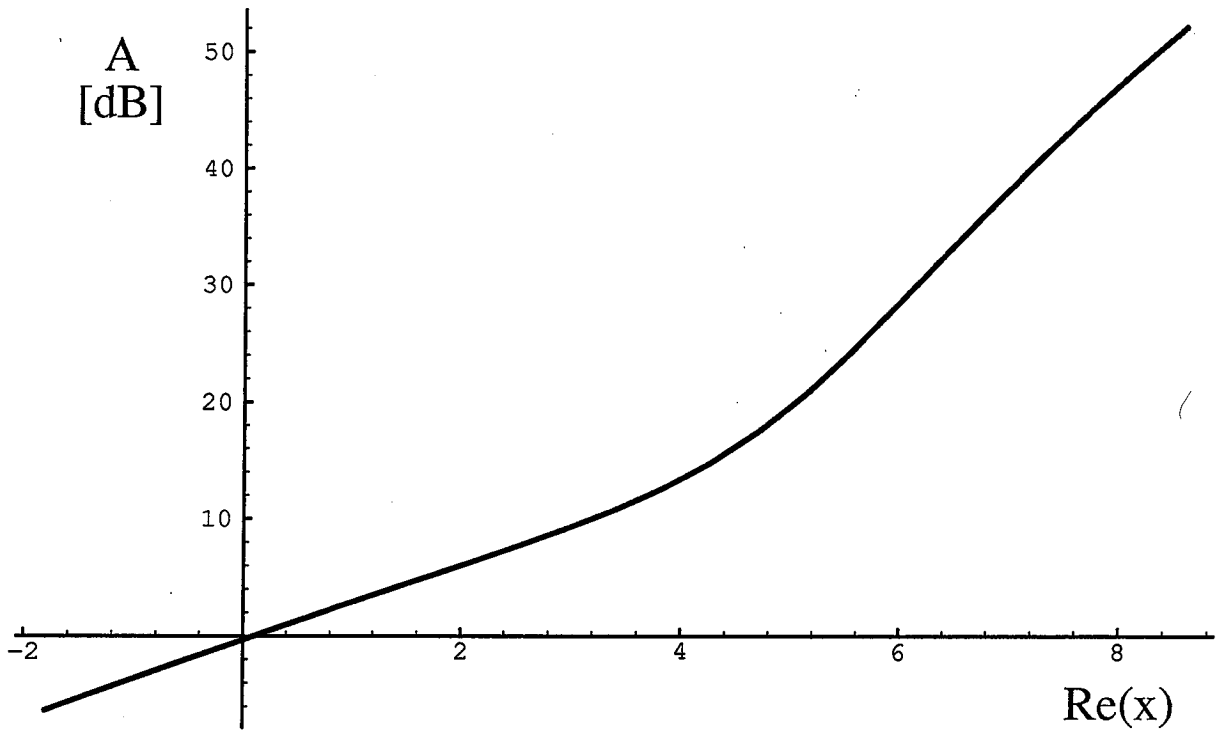

Fig. 4

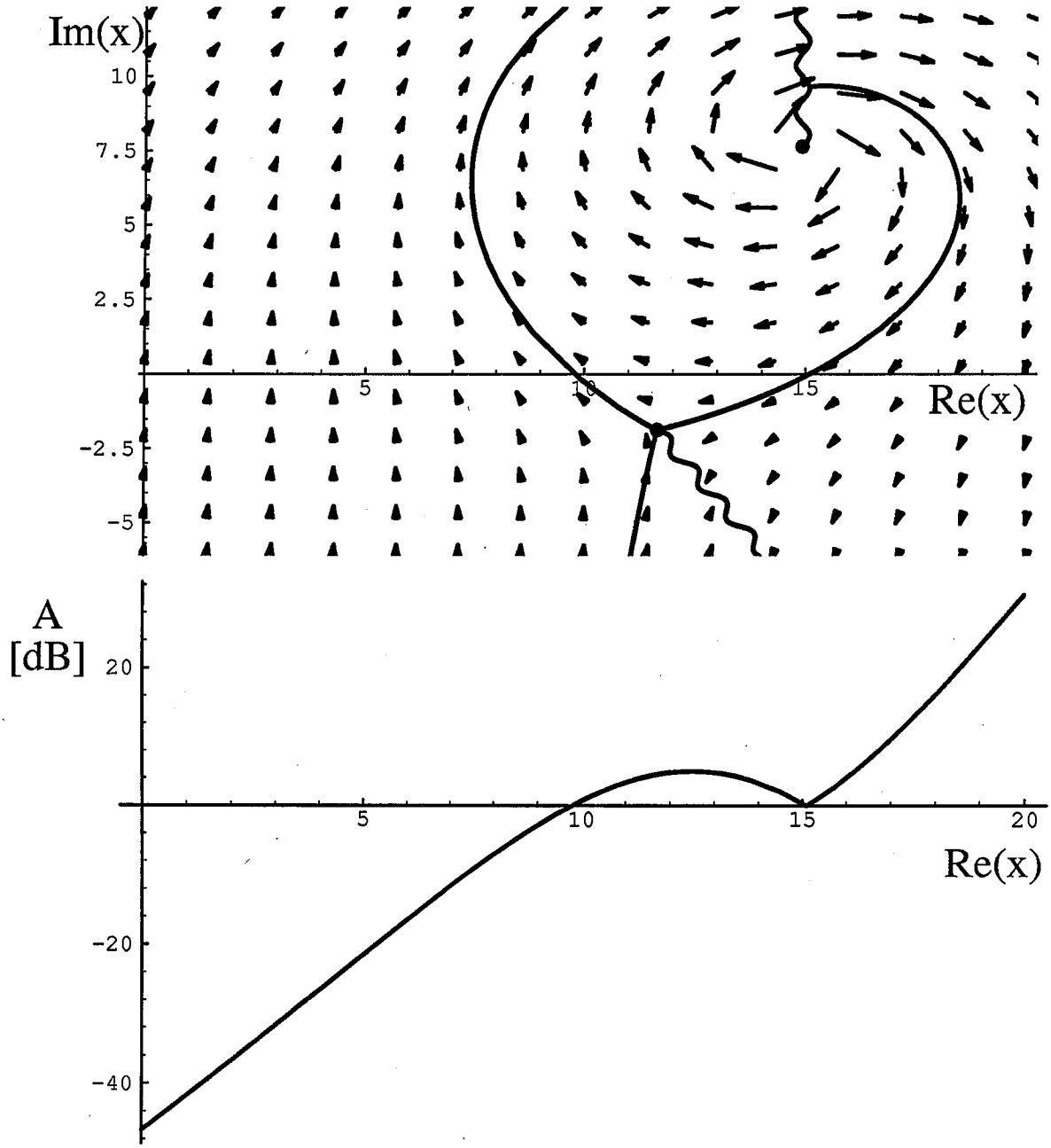

Fig. 5

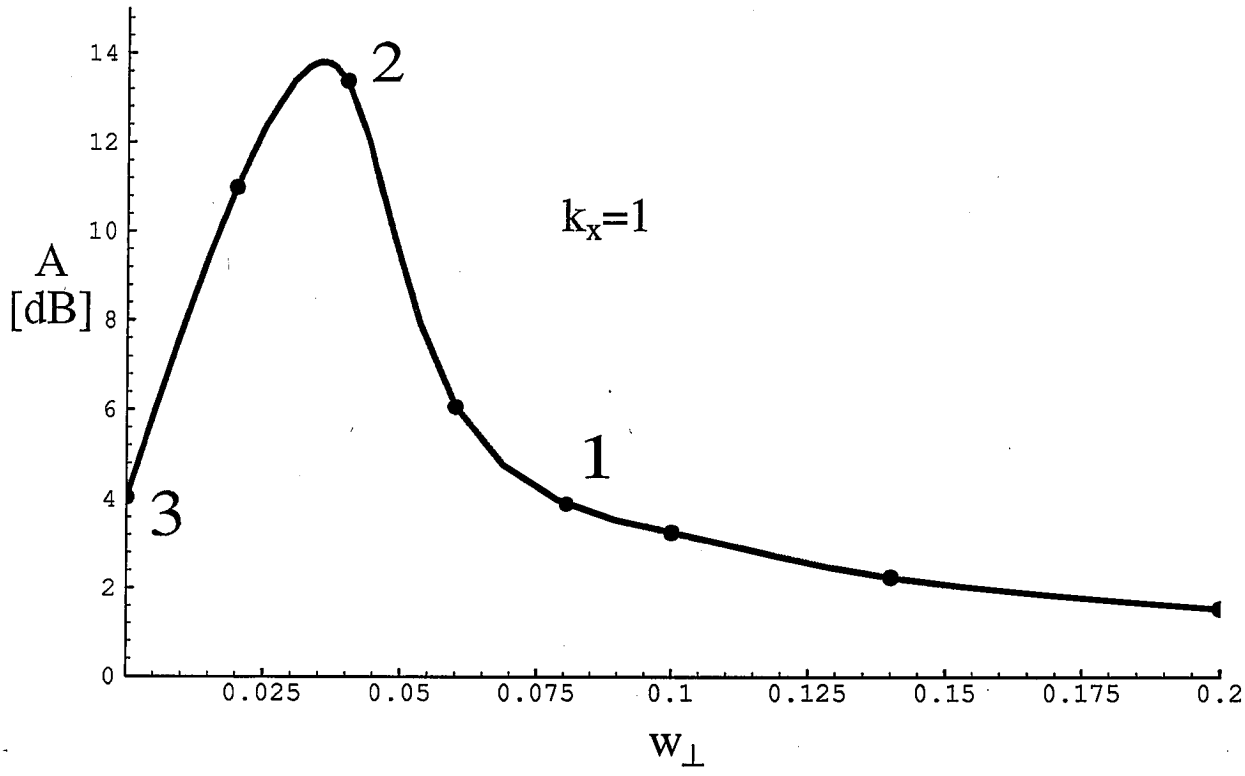
14
12
10
8
6
4
2
0
A
[dB]
2
1
3
k_x=1
0.025
0.05
0.075
0.1
0.125
0.15
0.175
0.2
$w_\perp$

Fig. 6

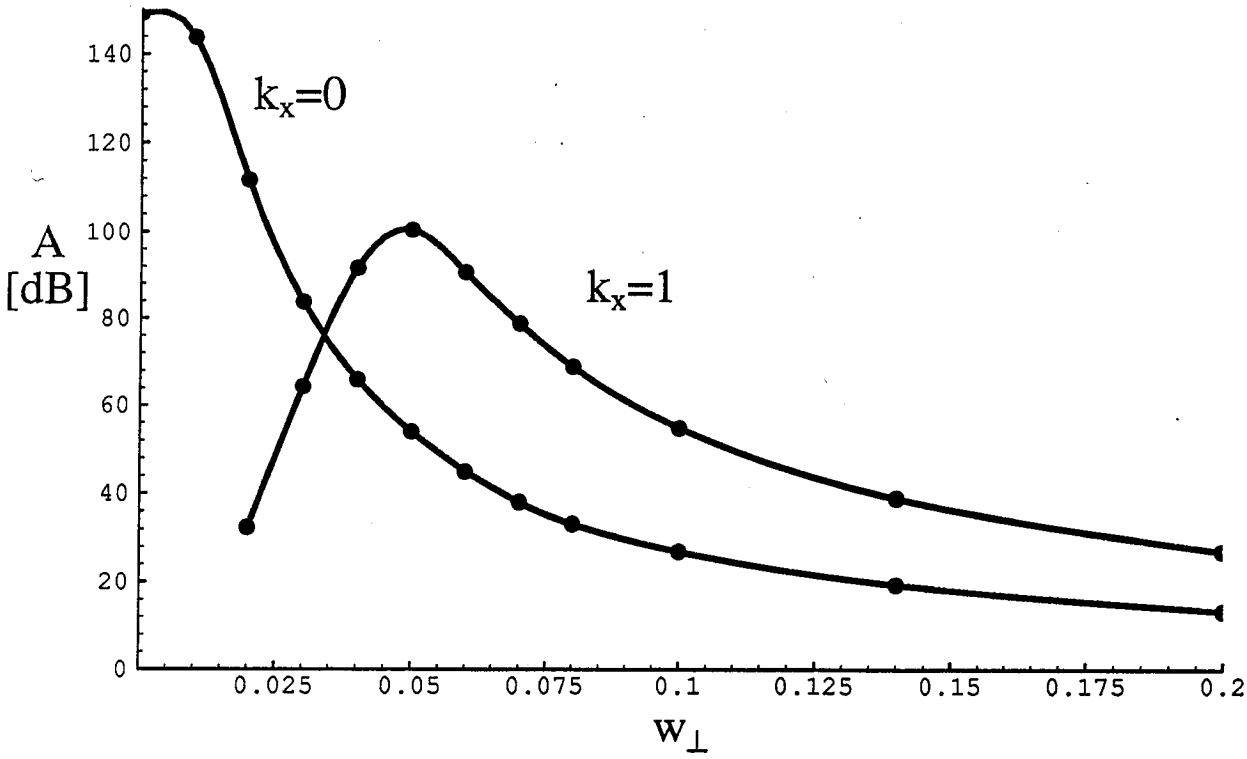
140
120
100
80
60
40
20
0
A
[dB]
k_x=0
k_x=1
0.025
0.05
0.075
0.1
0.125
0.15
0.175
0.2
$w_\perp$

Fig. 7